Electron beam-induced excitation rates in crystalline solids from first-principles

Anthony Yoshimura[1,2], Michael Lamparski[2], Joel Giedt[2], David Lingerfelt[3], Jacek Jakowski[3], Ganesh Panchapakesan[3], Tao Yu[4], Bobby Sumpter[4], and Vincent Meunier[2,5*]

[1] *Design Physics Division, Lawrence Livermore National Laboratory, Livermore, CA 94550, USA*
[2] *Department of Physics, Applied Physics, and Astronomy, Rensselaer Polytechnic Institute, Troy, New York 12180, USA*
[3] *Computational Sciences and Engineering Division, Oak Ridge National Laboratory, Oak Ridge, TN 37831, USA*
[4] *Department of Chemistry, University of North Dakota, Grand Forks, ND 58202, USA*
[5] *Department of Materials Science and Engineering, Rensselaer Polytechnic Institute, Troy, NY 12180, USA*
[*] *Correspondence to be addressed to meuniv@rpi.edu*

December 5, 2020

Abstract

The ability to control the structure of any material at the atomic-scale can provide powerful solutions to many of today's most pressing technological and environmental challenges. To this end, electron irradiation by transmission electron microscopy can be used to engineer the morphology of 2-dimensional (2D) materials with a high degree of spatial control. It follows that many computational models have been developed to predict the rates of atomic displacements in irradiated materials. However, while current models give reasonable predictions for conductors, they often drastically underestimate the displacement rates in insulators. This is because the majority of these methods focus solely on interactions between the beam electrons and target nuclei, neglecting the possibility of beam-induced electronic excitations. In insulators, these excitations can reduce the binding energies of the irradiated atoms, increasing their displacement rates. To address this phenomenon, this paper combines quantum electrodynamics with density functional theory to calculate the probability of beam-induced of excitation in 2D insulating crystals. We find that the probability of excitation induced by the transmission of a single 60 keV beam electron is about 16% in hexagonal boron nitride and 67% in molybdenum disulfide. These probabilities increase and approach unity as the beam energy approaches zero. Incorporating these probabilities into computational models reveals that appreciable sputtering can occur at beam energies much lower than we would otherwise expect, reducing the disparity between theory and experiment. This new predictive power would be a boon for materials engineers, allowing for the controlled manipulation of any 2D material for targeted functionality.

1

1 Introduction

A game a billiards involves two types of collisions: ball-to-ball and ball-to-table. In a ball-to-ball collision, the energy transfer from the moving ball to the stationary ball can be large because their masses are equal. It follows that a set of initially stationary balls are expected to rearrange after ball-to-ball collisions. One could call such collisions *inelastic*, since they cause the initially moving ball to lose a significant amount of its energy. On the other hand, very little energy is transferred in a ball-to-table collision, in which a moving ball strikes the rail of the table. This is because the mass of the table is much greater than that of the ball. As a result, the ball is expected to bounce off the rail without losing any velocity. In this way, one could call such a collision *elastic*, since the moving ball retains its energy.

In the case of a material under electron beam irradiation, electron-electron collisions liken to ball-to-ball, while electron-nuclear collisions liken to ball-to-table. As such we expect the material electrons to rearrange quite readily from an inelastic collision with the beam electron. This rearrangement comes in the form of electronic excitation. These beam-induced excitations are prevalent and consequential. They can affect the materials structural response to an irradiating electron beam.

1. There are a variety of structural responses that can take place under electron irradiation. In this work, we focus solely on *sputtering*, in which an atom is ejected from the material, leaving behind a vacancy. Sputtering results from electron-nuclear collisions. If the energy transferred to the nucleus is greater than its displacement threshold E_d, it will sputter.

2. critical energy is the minimum beam energy required to sputter an atom, assuming the atom is initially at rest.

3. 2D materials provide an excellent platform to track displacement rates under electron irradiation. 2D materials have many distinct and interesting properties. They are also a perfect platform to test displacement cross sections.

Defects in materials are interesting. While defects will almost certainly destroy the properties of the pristine material, they can vastly extend the the space of possible applications. Electron irradiation by transmission electron microscopy (TEM) is an effective method for engineering the properties and morphology of an irradiated material with sub-angstrom precision via selective atomic displacement [**Zhao2017**, **Schleberger2018**, **Oxley2014**, **Kretschmer2018**, **Komsa2013**]. Many computational models have been proposed to predict electron beam-induced displacement rates in 2D materials [**Meyer2012**, **Susi2016**, **Yoshimura2018**, **Susi2019**]. However, the vast majority of current methods focus solely on interactions between the beam electrons and target nuclei, neglecting any coupling with the material's electrons. Thus, while present-day models give reasonable predictions for conductors, where electronic relaxation is rapid, they often vastly underestimate the atomic displacement rates in insulators. For example, boron has been shown to sputter from hexagonal boron nitride (hBN) under irradiation that is about half of the calculated critical energy [**Susi2019**, **Cretu2015**]. Furthermore, Se sputters from WSe_2 under irradiation of 60 keV, almost 150 keV below its predicted critical energy [**Lin2015**]. Perhaps even more surprising is that chalcogen sputtering rates in MoS_2 and $MoSe_2$ were observed to be about equal under 80 keV irradiation [**Lehnert2017**],

despite Se being more than two times heavier than S. Discrepancies in semiconductors like these severely inhibit the use of TEM for materials engineering, as electronic energy gaps are the foundation of electronic and photoelectric device technology.

These results suggest that the displacement thresholds in insulating crystals are much smaller than what is predicted by ground state DFT. Lehnert et al. [**Lehnert2017**] have proposed that the consideration of inelastic scattering, i.e., beam-induced electron excitation, can lead to a reduction in E_d. This would increase the sputtering rates and enable sputtering under beam energies well-below the ground state critical energy. In light of this, this work combines quantum electrodynamics (QED) and density functional theory (DFT) to derive the probability of beam-induced excitation in 2D insulating crystals. DFT can provide effective single particle states that can be decomposed into a plane wave basis [**Hohenberg1964**, **Kohn1965**, **Kresse1996a**], while QED is well-equipped to describe how each plane wave evolves in time through interactions with an electromagnetic field [**Peskin1995**, **Lancaster2014**]. Thus, a plane wave decomposition of the Kohn-Sham orbitals can allow for a component-by-component treatment of the interactions between the beam and material electrons. This generalized QED-DFT approach will enable, for the first time, a first-principles description of any beam-matter interaction process, with the only approximation being the order in the fine-structure constant to which the time-evolution operator is expanded. This paper is divided into two sections: First, we derive the probability of an excitation for a 2D insulating crystal as a function of beam energy. Second, we show how this excitation probability can be used to predict sputtering rates in insulators.

2 Probability of beam-induced excitation

The sputtering of an excited atom hinges on three successive processes. (1) A beam electron excites n ground state electrons to unoccupied states. (2) The energy E_t transferred to that atom's nucleus by the beam electron is greater than the displacement threshold $E_d(n)$, which depends on the number of excitations (3) The excited electron remains excited long enough for the target atom to leave the vicinity of its original site. Thus, the total sputtering cross section can be written as

$$\sigma(\text{sputtering}) = P_{\text{ex}}(E_b) \times P(\text{still excited}) \times \sigma\left(E_t > E_d(n)\right). \qquad (1)$$

The method for calculating $P(E_t > E_d)$ for a given temperature well-established in the literature [**Meyer2012**, **Susi2016**, **Yoshimura2018**]. Meanwhile, first-principles methods for calculation of $P(\text{still excited})$ have already been established, and often, experimental data can be used to determine the excitation lifetimes in a material. Therefore, this section focuses on how to obtain $P(\text{excitation})$ by combining QED and DFT.

In a ground state crystal, an occupied electron energy eigenstate has zero overlap with any unoccupied state. As energy eigenstates are stationary, this means that an electron in an occupied state will never be measured in an excited state if left unperturbed. However, the collision of a beam electron can give an occupied state a momentum boost that breaks its orthogonality with the unoccupied states. Thus, the boosted ground state state has a nonzero probability of being measured in an excited state. This is the basic mechanism of beam-induced excitation.
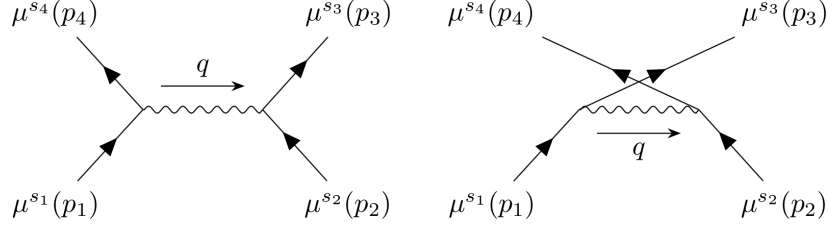
Figure 1: The lowest order electron-electron scattering perturbation includes two Feynmann diagrams: the t-channel (left) and the u-channel (right).

With this in mind, the method for deriving the excitation probability proceeds as follows: First, determine the amplitude for a free electron to scatter from one momentum eigenstate into another after collision with another free electron. Second, obtain the amplitude for scattering from one wavepacket into another by summing over the amplitudes for each momentum component of one wave packet to scatter into each momentum component of the other. Third, decompose a pair of occupied and unoccupied crystal states into a momentum basis and plug them in as the incoming and outgoing wave packets respectively. Square the amplitude to obtain the corresponding excitation probability Finally, find the probability of not exciting any transitions and subtract that probability from unity. The result is the probability of exciting at least one crystal electron.

2.1 Scattering of free electrons

We first derive the scattering amplitude for momentum transfer between two free electrons. Going forward, we label the 4-momenta of the incoming electrons as p_1 and p_2, while the outgoing electrons have momenta p_3 and p_4. The 4-momentum of the nth electron can be written as $p_n = (\epsilon_n, p_n^x, p_n^y, p_n^z) = (\epsilon_n, \mathbf{p}_n)$ where ϵ_n is the particle's energy and $\mathbf{p}_n$ is its 3-momentum. Dot products between 4-vectors are taken over Minkowski space, i.e. $p_n \cdot p_m = g_{\mu\nu}p_n^\mu p_m^\nu = \epsilon_n\epsilon_m - \mathbf{p}_n \cdot \mathbf{p}_m$, where $\mathbf{p}_n \cdot \mathbf{p}_m = p_n^x p_m^x + p_n^y p_m^y + p_n^z p_m^z$.

To lowest order, the amplitude for free electron scattering can be represented by two tree-level diagrams, which we call the t- and u-channels (figure 1). Using Feynman's rules, we can write these diagrams in terms of Dirac spinors, yielding the invariant matrix element

$$
\begin{aligned}
\mathcal{M}(p_4 p_3 \leftarrow p_2 p_1) = \frac{e^2}{2} \sum_{s_1}\sum_{s_2}\sum_{s_3}\sum_{s_4} & \\
\left[\bar{u}^{s_4}\left(p_4\right)\gamma^\mu u^{s_1}\left(p_1\right)\left(\frac{1}{p_3 - p_2}\right)^2 \bar{u}^{s_3}\left(p_3\right)\gamma_\mu u^{s_2}\left(p_2\right) \right. & \\
\left. + \bar{u}^{s_3}\left(p_3\right)\gamma^\mu u^{s_1}\left(p_1\right)\left(\frac{1}{p_4 - p_2}\right)^2 \bar{u}^{s_4}\left(p_4\right)\gamma_\mu u^{s_2}\left(p_2\right) \right] &
\end{aligned}
\tag{2}
$$

where $s_n = 1$ or 2 denotes the spin of the nth electron. The factor of $1/2$ before the summation arises from the assumption that the incoming states are unpolarized. The last line of equation (2) defines the invariant matrix element $\mathcal{M}$. The evaluation of

4

$\mathcal{M}$ in terms of the components of the electron 4-momenta is straightforward, though cumbersome, and is described in section **??**.

The momentum transfer is $p_3 - p_2$ for the t-channel and $p_4 - p_2$ for the u-channel. Because the DFT cutoff energy is much smaller than the beam energy, we only consider momentum transfers that are much smaller than p_1. This means that one channel is always much bigger than the other. Taking advantage of the indistinguishibility of the electrons, we calculate only the t-channel and multiply by 2 to obtain $\mathcal{M}$.

We can use $\mathcal{M}$ to quickly obtain the scattering amplitude between two free electrons

$$\langle p_4 p_3 | \hat{T} | p_2 p_1 \rangle = (2\pi)^4 \delta(p_1 + p_2 - p_3 - p_4) \mathcal{M}(p_4 p_3 \leftarrow p_2 p_1), \tag{3}$$

where $\hat{T}$ is the scattering operator.

2.2 Scattering of wavepackets

We can now determine the amplitude for the scattering of two arbitrary electron states ϕ_1 and ϕ_2 into ϕ_3 and ϕ_4.

$$\langle \phi_4 \phi_3 | \hat{T} | \phi_2 \phi_1 \rangle = \int \frac{d^3 p_4 d^3 p_3 d^3 p_2 d^3 p_1}{(2\pi)^{12} 16 \epsilon_4 \epsilon_3 \epsilon_2 \epsilon_1} \langle \phi_4 \phi_3 | p_4 p_3 \rangle \langle p_4 p_3 | \hat{T} | p_2 p_1 \rangle \langle p_2 p_1 | \phi_2 \phi_1 \rangle \tag{4}$$

On the right side, we have inserted two resolutions of the identity given in equation (**??**) in the SI. By inserting equation (3), the amplitude can be written in terms of the invariant matrix element $\mathcal{M}$, becoming

$$\int \frac{d^3 p_4 d^3 p_3 d^3 p_2 d^3 p_1}{(2\pi)^{12} 16 \epsilon_4 \epsilon_3 \epsilon_2 \epsilon_1} \langle \phi_4 | p_4 \rangle \langle \phi_3 | p_3 \rangle \langle p_2 | \phi_2 \rangle \langle p_1 | \phi_1 \rangle$$
$$\times \mathcal{M}(p_4 p_3 \leftarrow p_2 p_1)(2\pi)^4 \delta(p_1 + p_2 - p_3 - p_4). \tag{5}$$

We can use the delta function to integrate over $\mathbf{p}_4$ and p_3^z, yielding

$$\int \frac{d^2 p_3^\perp d^3 p_2 d^3 p_1}{(2\pi)^8 16 \epsilon_2 \epsilon_1} \frac{\mathcal{M}(p_4 p_3 \leftarrow p_2 p_1)}{|p_3^z \epsilon_4 - p_4^z \epsilon_3|} \langle \phi_4 | p_4 \rangle \langle \phi_3 | p_3 \rangle \langle p_2 | \phi_2 \rangle \langle p_1 | \phi_1 \rangle, \tag{6}$$

where it is understood that p_4 and p_3 satisfy $p_1 + p_2 = p_3 + p_4$. The normalization of 3-momentum states defined equation (**??**) allows us to rewrite the expression as

$$\int \frac{d^2 p_3^\perp d^3 p_2 d^3 p_1}{(2\pi)^8} \sqrt{\frac{\epsilon_4 \epsilon_3}{\epsilon_2 \epsilon_1}} \frac{\mathcal{M}(p_4 p_3 \leftarrow p_2 p_1)}{4 |p_3^z \epsilon_4 - p_4^z \epsilon_3|} \langle \phi_4 | \mathbf{p}_4 \rangle \langle \phi_3 | \mathbf{p}_3 \rangle \langle \mathbf{p}_2 | \phi_2 \rangle \langle \mathbf{p}_1 | \phi_1 \rangle. \tag{7}$$

We can then discretize the momenta by replacing $d^3 p_i / (2\pi)^3 \to V^{-1}$ and $d^2 p_i^\perp / (2\pi)^2 \to A^{-1}$, where V and A are the volume and cross sectional area of the simulated crystal, i.e., the volume and cross sectional area of the unit cell times the number of k-points in the cell. With this, the amplitude becomes

$$\frac{1}{AV^2} \sum_{\mathbf{p}_3^\perp} \sum_{\mathbf{p}_2} \sum_{\mathbf{p}_1} \sqrt{\frac{\epsilon_4 \epsilon_3}{\epsilon_2 \epsilon_1}} \frac{\mathcal{M}(p_4 p_3 \leftarrow p_2 p_1)}{4 |p_3^z \epsilon_4 - p_4^z \epsilon_3|} \langle \phi_4 | \mathbf{p}_4 \rangle \langle \phi_3 | \mathbf{p}_3 \rangle \langle \mathbf{p}_2 | \phi_2 \rangle \langle \mathbf{p}_1 | \phi_1 \rangle. \tag{8}$$

We are now ready to replace $|\phi_1\rangle$, $|\phi_2\rangle$, $|\phi_3\rangle$, and $|\phi_4\rangle$ with states relevant to electron beam-induced excitation.

5

2.3   probability of crystal excitations

We now consider the specific case of beam-induced excitations to determine the form of the four electron states in equation (8). We assign $|\phi_1\rangle$ and $|\phi_4\rangle$ to the initial and final beam states $|p_b\rangle$ and $|p'_b\rangle$ respectively. States $|\phi_2\rangle$ and $|\phi_3\rangle$ are then the ground and excited crystal states $|n\mathbf{k}\rangle$ and $|n\mathbf{k}'\rangle$ respectively. The excitation amplitude becomes

$$\langle p'_b, n'\mathbf{k}'|\hat{T}|n\mathbf{k}, p_b\rangle = \frac{1}{AV^2}\sum_{\mathbf{p}_3^\perp}\sum_{\mathbf{p}_2}\sum_{\mathbf{p}_1}\sqrt{\frac{\epsilon_4\epsilon_3}{\epsilon_2\epsilon_1}}\frac{\mathcal{M}(p_4p_3\leftarrow p_2p_1)}{4|p_3^z\epsilon_4 - p_4^z\epsilon_3|}$$

$$\times \langle \mathbf{p}'_b|\mathbf{p}_4\rangle\langle n'\mathbf{k}'|\mathbf{p}_3\rangle\langle \mathbf{p}_2|n\mathbf{k}\rangle\langle \mathbf{p}_1|\mathbf{p}'_b\rangle. \tag{9}$$

The zeroth components of the initial and final beam momenta obey the free particle dispersion relations, so that $\epsilon_1 = \sqrt{|\mathbf{p}_1|^2 + m^2}$. and $\epsilon_4 = \sqrt{|\mathbf{p}_4|^2 + m^2}$. Meanwhile, the momentum of the crystal states can be treated nonrelativistically. Thus, the zeroth components of the crystal state momenta are the energy eigenvalues of their crystal states plus the electron rest mass, i.e., $\epsilon_2 = \epsilon_{n\mathbf{k}} + m$ and $\epsilon_3 = \epsilon_{n'\mathbf{k}'} + m$.

We can now evaluate the overlaps in equation (9). The initial beam state is highly localized on $\mathbf{p}_b$, meaning that

$$|\langle \mathbf{p}_1|\mathbf{p}_b\rangle|^2 = V\delta_{\mathbf{p}_1,\mathbf{p}_b} \quad\Rightarrow\quad \langle \mathbf{p}_1|\mathbf{p}_b\rangle = V^{1/2}\delta_{\mathbf{p}_1,\mathbf{p}_b}. \tag{10}$$

Meanwhile, the ground and excited crystal states can be written as

$$|n\mathbf{k}\rangle = V^{-1/2}\sum_{\mathbf{G}}C_{\mathbf{G}+\mathbf{k}}^n|\mathbf{G}+\mathbf{k}\rangle$$

$$|n'\mathbf{k}'\rangle = V^{-1/2}\sum_{\mathbf{G}'}C_{\mathbf{G}'+\mathbf{k}'}^{n'}|\mathbf{G}'+\mathbf{k}'\rangle, \tag{11}$$

meaning that

$$\langle \mathbf{p}_2|\phi_2\rangle = \langle \mathbf{G}+\mathbf{k}|n\mathbf{k}\rangle = V^{1/2}C_{\mathbf{G}+\mathbf{k}}^n$$

$$\langle \mathbf{p}_3|\phi_3\rangle = \langle \mathbf{G}'+\mathbf{k}'|n'\mathbf{k}'\rangle = V^{1/2}C_{\mathbf{G}'+\mathbf{k}'}^{n'}. \tag{12}$$

Lastly, we do not care where the outgoing scattered electron ends up, so we wish for $|\mathbf{p}'_b\rangle$ to satisfy

$$|\langle \mathbf{p}_4|\mathbf{p}'_b\rangle|^2 = V \quad\Rightarrow\quad \langle \mathbf{p}_4|\mathbf{p}'_b\rangle = V^{1/2}. \tag{13}$$

The excitation amplitude is then obtained by plugging in the overlaps from equations (10), (12), and (13) into expression (8).

$$\boxed{\langle p'_b, n'\mathbf{k}'|\hat{T}|n\mathbf{k}, p_b\rangle = \frac{1}{A}\sum_{\mathbf{G}'^\perp}\sum_{\mathbf{G}}\sqrt{\frac{\epsilon_4\epsilon_3}{\epsilon_2\epsilon_1}}\frac{\mathcal{M}(p_4p_3\leftarrow p_2p_1)}{4|p_3^z\epsilon_4 - p_4^z\epsilon_3|}C_{\mathbf{G}'+\mathbf{k}'}^{n'*}C_{\mathbf{G}+\mathbf{k}}^n,} \tag{14}$$

where it is understood that $p_2 = (\epsilon_{n\mathbf{k}}, \mathbf{G}+\mathbf{k})$ and $p_3 = (\epsilon_{n'\mathbf{k}'}, \mathbf{G}'+\mathbf{k}')$, and p_4 and p_3^z satisfy $p_1 + p_2 = p_4 + p_3$. Squaring this amplitude yields the probability of a single electron excitation from the valence band state $|n\mathbf{k}\rangle$ to the conduction band state $|n'\mathbf{k}'\rangle$,

$$P(n'\mathbf{k}' \leftarrow n\mathbf{k}) = \left|\langle p'_b, n'\mathbf{k}'|\hat{T}|n\mathbf{k}, p_b\rangle\right|^2 \tag{15}$$

	displacement threshold (eV)			
# excitations	0	1	2	3
hBN	15.77	11.44	6.721	1.939
MoS_2	6.735	5.077	3.377	1.706

Table 1: The displacement thresholds of single hBN and MoS_2 decrease as the number of excitations increase

2.4   Total excitation probability

Finally, to determine the probability of a beam-induced excitation from *any* valence band state to *any* conduction band state, we multiply the probabilities of "missing" all state-to-state excitations for all pairs of occupied and unoccupied states and subtract that product from unity. Thus, the probability that a beam electron will induce any electronic excitation in the material is

$$P(\text{excitation}) = 1 - \prod_{\mathbf{k'}} \prod_{\mathbf{k}} \prod_{n' \in \mathcal{C}} \prod_{n \in \mathcal{V}} \left[1 - P(n'\mathbf{k'} \leftarrow n\mathbf{k})\right], \tag{16}$$

where $\mathbf{k}$ and $\mathbf{k'}$ run over all k-points, n over occupied valence bands, and n' over unoccupied conduction bands. Specifically,

$$\begin{aligned} \mathcal{V} &= \{n | \epsilon_{n\mathbf{k}} < \epsilon_F\} \\ \mathcal{C} &= \{n' | \epsilon_F < \epsilon_{n'\mathbf{k'}} < \Phi\}, \end{aligned} \tag{17}$$

where ϵ_F is the Fermi level and Φ is the work function.

3   Sputtering cross section

The sputtering cross section describes the likelihood that a beam electron can transfer enough energy to a target nucleus to cause it to sputter. The McKinley and Feshbach cross section has been shown to work well for conducting materials comprised of light elements.

$$\sigma_{\text{tot}}(E_b) = \left[1 - \sum_{n=1}^{3} P(E_b)^n\right] \sigma\left(E_d(n=0)\right) + \sum_{n=1}^{3} P(E_b)^n \sigma\left(E_d(n)\right) \tag{18}$$

Things to discuss

1. As the target atom is displaced, the occupied CBM state sinks into the gap and localizes on the displaced atom[**Kretschmer2020**].

2. the excitation lifetime of hBN is 0.75 ns[**Li2016b**]. We can therefore expect that the excitation always lives long enough to reduce the displacement threshold of the affected atom. The excitation lifetime of MoS_2 is much shorter, on the order of a few picoseconds[**Korn2011**, **Lagarde2014**, **Palummo2015**]. Nonradiative pathways are faster than radiative pathways[**Shi2013**], so always assume
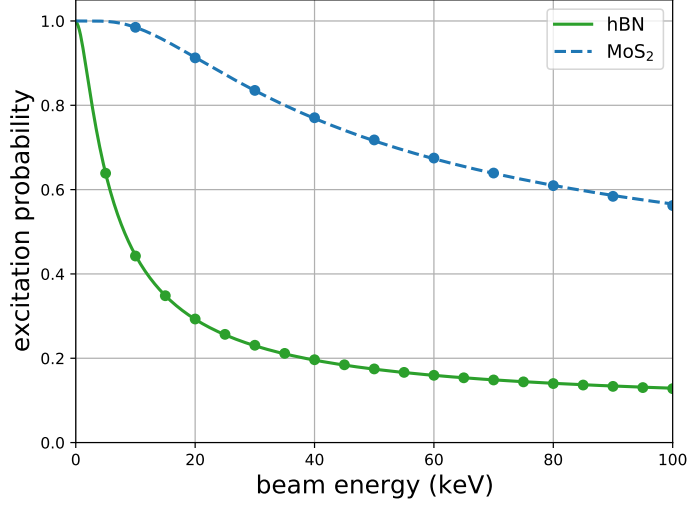
Figure 2: The excitation probability decreases with increasing beam energy. MoS_2 has a larger excitation probability than hBN does because it has a smaller band gap and more valence states.

that the excited electron is at the HOMO while the hole is at the LUMO. A sputtered sulfur atom takes less than a pico second to leave the vicinity of its pristine site[**Yoshimura2018**]. Therefore, we can estimate the likelihood that a beam-induced excitation will facilitate a sputtering event using

$$P(\text{still excited}) = e^{-t/\tau} \tag{19}$$

where τ is the excitation lifetime. Are non-radiative pathways more important?

3. field theory has been laid out, but it has never been applied to materials

4. time evolution operator should account for potential

5. excitation probability is inversely proportional to band gap squared

6. If $P \ll 1$, the excitation probability is inversely proportional to beam energy, as predicted by Bethe[**Kretschmer2020**]. multiple excitations are likely at low beam energies.

7. The excitation probability is inversely proportional to the square of the band gap

8. hBN armchair edges are more likely to form[**Cretu2015**]

9. excitation probabilities should change with the presence of defects

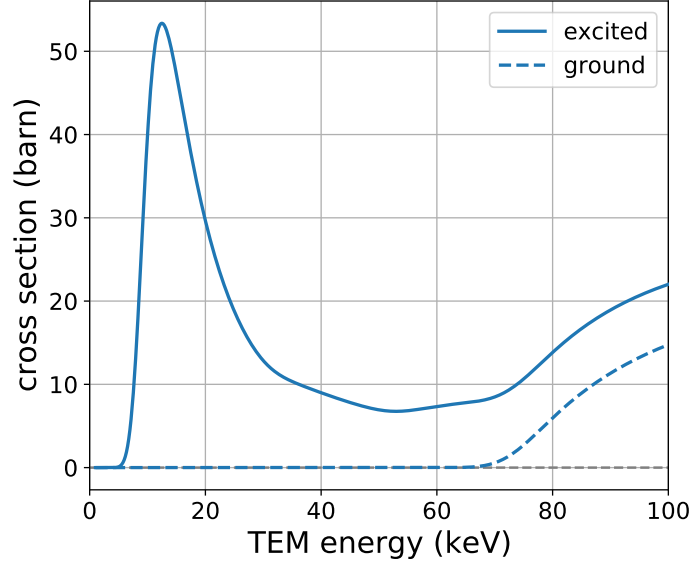10. nonadiabatic electronic evolution can change both the relaxation time τ and the displacement threshold E_b.

Figure 3: Beam-induced excitations in hexagonal boron nitrice (hBN) cause the sputtering rate to peak at beam energies well-below the ground state critical energy. The dashed line shows the sputtering cross section for ground state hBN, while the solid line accounts for up to three excitations. A temperature of 300 K was assumed.

11. as we do now the precise relaxation pathway, we plot the sputtering cross section for several values of τ along with the experimental date (figure 3)

4   Conclusion

For a given electron beam energy, the sputtering rate is much greater than what is currently predicted by ground state models. We combine QED scattering theory with DFT orbitals to determine the likelihood of beam induced excitation. We then show how this excitation probability to calculate the sputtering cross section in hBN in MoS_2.

There is room for several improvements to calculating the probability of subsequent excitations.

1. Accommodate PAW and ultrasoft pseudopotentials, in the same way done in [**Shishkin2006a**, **Gajdos2006**, **Paier2005**].

2. Calculate excited state plane wave coefficients self-consistently using constrained DFT.

3. consider core excitations and second order electonic excitation effects. Core excitations are less likely to affect sputtering rates since they have shorter lifetimes and a smaller excitation probability due to the much larger excitation energy.

4. Include ionization and other electronic responses

5. spin polarization effects can be accounted for by making $\mathcal{M}$ spin-dependent. That is, not averaging over spins as is done in equation (2)

6. excitations are likely correlated, so that the excitation probability depends on the specific excitations that have already occured.

7. better treatment of excitation dynamics[**Kretschmer2020**] and relaxation pathways[].

8. In the case of atomic displacement, the beam electron path changes significantly after collision with the nucleus. This new path would produce a different excitation probability.

9. different electronic relaxation pathways[**Lagarde2014**, **Kozawa2014**, **Nie2015**, **Shi2013a**]

5 Methods

Density functional theory (DFT)[**Hohenberg1964**, **Kohn1965**] was used to determine electronic and ionic structure for all materials from first-principles. Relaxation calculations were carried using the Vienna ab initio Simulation Package (VASP)[**Kresse1996**, **Kresse1996a**] using the projector augmented wave method (PAW)[**Blochl1994**]. The plane wave coefficients $C_{\mathbf{G}+\mathbf{k}}^n$ were obtained with Quantum ESPRESSO[**Giannozzi2009**] utilizing optimized norm-conserving Vanderbilt pseudopotentials[**Hamann2013**, **Schlipf2015**].

Because condition (**??**) relies on the orthogonality of our Kohn-sham orbitals, the optimized norm-conserving Vanderbilt pseudopotentials[**Hamann2013**, **Schlipf2015**] were used to determine all plane wave coefficients. It is of course possible to extend this method to ultrasoft and projector augmented wave (PAW) [**Blochl1994**] pseudopotentials using methods laid out in the literature[**Shishkin2006a**, **Gajdos2006**, **Paier2005**].

6 Acknowledgements